

Why experiments fail to detect the finite linear Rashba spin-orbit coupling of two-dimensional holes in semiconductor quantum wells: The case of Ge/SiGe quantum wells

Jia-Xin Xiong^{1,2}, Yang Liu^{1,2}, Shan Guan^{1,*}, Jun-Wei Luo^{1,2,†} and Shu-Shen Li^{1,2}

¹State Key Laboratory of Superlattices and Microstructures, Institute of Semiconductors, Chinese Academy of Sciences, Beijing 100083, China

²Center of Materials Science and Optoelectronics Engineering, University of Chinese Academy of Sciences, Beijing 100049, China



(Received 29 July 2022; revised 29 September 2022; accepted 11 October 2022; published 24 October 2022)

The magnetotransport experiments based on the weak antilocalization (WAL) effect have confirmed the common belief that the Rashba spin-orbit coupling (SOC) of two-dimensional (2D) holes in semiconductor quantum wells (QWs) is a k -cubic term as the lowest order with negligible linear terms. However, an emerging finite linear Rashba SOC was recently found in 2D holes by semiempirical pseudopotential method (SEPM) due to the direct dipolar coupling of an external electric field to the valence subbands in the presence of heavy-hole–light-hole (HH-LH) mixing. Here, we resolve this discrepancy by illustrating that the hole densities in the experiments are so high that the emerging linear term becomes undetectable since its strength declines substantially as increasing the wavevector k . Taking the example of a strained Ge/Si_{0.5}Ge_{0.5} QW utilized in the experiment [*Phys. Rev. Lett.* **113**, 086601 (2014)], we demonstrate that the hole density must be reduced by a factor of 5 to below $2.1 \times 10^{11} \text{cm}^{-2}$ in order to probe the k -linear term. We also evaluate the possibility to achieve WAL at low hole densities in order to measure SOC. These findings shed new light on the experimental measurement of Rashba SOC.

DOI: [10.1103/PhysRevB.106.155421](https://doi.org/10.1103/PhysRevB.106.155421)

I. INTRODUCTION

Rashba spin-orbit coupling (SOC) is a k -dependent relativistic effect entangling the spin and orbital degrees of freedom, manifesting as the spin splitting of energy bands in terms with odd powers of k as required by the time-reversal invariance [1–3]. It was believed that, in 2D heterostructures, the Rashba SOC of conduction subbands and light hole (LH) subbands are k -linear terms as the leading order, whereas heavy hole (HH) subbands possess a tiny k -linear term [2–4]. Thus, in 2D holes, the k -cubic term was usually regarded as the lowest-order term of the Rashba SOC [2,3,5,6]. This is because the carrier density in most applications is so low that the Fermi wavevector k_F is in a small k range where a finite k -linear term, if existing, will usually overwhelm the cubic term. On the other hand, the k -linear and k -cubic Rashba SOC differ strikingly, e.g., in their effective magnetic fields and resulting spin-momentum locking-induced spin textures [7]. Although a third-order k -linear Rashba SOC originating from the anisotropic coupling between bonding and antibonding p -orbital states was proposed [2,3], it can be neglected due to its less than 1% contribution to the total spin splitting [4]. The absence of k -linear Rashba SOC in HH subbands prevents 2D holes from many potential applications in spintronics [6,8–16] until we recently found a first-order k -linear Rashba SOC, called the direct Rashba SOC, in 2D holes based on the semiempirical pseudopotential method (SEPM), originating from the heavy-hole–light-hole (HH-LH) mixing in a combi-

nation of a direct dipolar subband coupling [17]. For instance, this k -linear Rashba SOC supplies a theoretical foundation for experimentally achieved fast manipulation of hole spin qubits confined in Ge/SiGe quantum wells (QWs) [18–20]. Despite the emergent k -linear Rashba SOC being relatively weak (with respect to its electron counterpart) with a small linear Rashba parameter $\alpha_R = 2.0 \text{ meV \AA}$, it, and only it, can offer a high Rabi frequency of 108 MHz [21] achieved in the experiment [19]. It provides efficiently the admixture of the spin-opposite states with magnitude depending linearly on α_R of the electric dipole transitions for the electric dipole spin resonance (EDSR) in a hole spin qubit. This weak k -linear Rashba SOC can be further enhanced by increasing the external electric field and Ge well width, decreasing the in-plane biaxial strain, and engineering the barrier potential [17,21,22]. Particularly, the strongest linear Rashba SOC with strength exceeding 120 meV \AA was found in the [110]-oriented Ge QWs [23].

However, this k -linear Rashba SOC of 2D holes in QWs has never been probed in previous experimental measurements. Instead, experiments can only detect the k -cubic Rashba SOC, e.g., in Ge QWs, via the magnetotransport process [24,25] or the Shubnikov–de Haas (SdH) effect [26–28], in agreement with the previous common belief [2,3,5,6]. It is a puzzle why experiments fail to probe the recently theoretically proposed k -linear Rashba SOC.

In this work, we uncover that the discrepancy arises from the high k -dependence of the Rashba SOC in 2D holes, which manifests as the finite Rashba parameter of the k -linear term obtained in the extremely small k -range becoming negligible as the Fermi wavevector k_F moves away from the $\bar{\Gamma}$ -point. Whereas, the hole densities involved in all exper-

*shan_guan@semi.ac.cn

†jwluo@semi.ac.cn

TABLE I. Summary of typical values of quantities in experiments with only k -cubic Rashba parameters detected at a high hole density in Ge QWs [24–29].

Reference	k -cubic Rashba parameter γ_R (eVÅ ³)	Hole density n_h (10 ¹¹ cm ⁻²)	Fermi wavevector k_F ($\frac{2\pi}{a}$)	Ge well width (nm)		Compressive strain in Ge layers (%)	Method
				Alloy barrier			
Ref. [24]	20	10	0.022	20	Si _{0.5} Ge _{0.5}	2.1	WL-WAL
Ref. [25]	30	6	0.017	24	Si _{0.15} Ge _{0.85}	0.6	WL-WAL
Ref. [26]	100	5.9	0.017	11	Si _{0.2} Ge _{0.8}	0.8	SdH
Ref. [27]	100	4	0.014	22	Si _{0.2} Ge _{0.8}	0.8	SdH
Ref. [28]	100	5.9	0.017	11	Si _{0.2} Ge _{0.8}	0.8	SdH
Ref. [29]	50, 120	5.9, 2	0.017, 0.010	11, 22	Si _{0.2} Ge _{0.8}	0.8	Cyclotron resonance

imental measurements (summarized in Table I) are in the range of 0.010 - $0.022 \times (\frac{2\pi}{a})$ [24–29], giving rise to Fermi wavevectors k_F in the k -range where the k -linear term is almost vanished and leaving behind k -cubic term as the leading term. To directly compare with experimental measurements [24], we first calculate the spin splitting of energy subbands in strained Ge QWs using the SEPM. We then investigate the characteristics of the conductivity change by varying the fitting parameters and clarify how the weak localization (WL) and weak antilocalization (WAL) regions change with these parameters. We also illustrate that one has to increase the k -linear Rashba SOC for its detection in the WAL region at low hole densities.

II. DISPERSION OF SPIN SPLITTING: k -DEPENDENT RASHBA PARAMETERS

Considering that the QW structure adopted in the experiment [24] has a 20 nm thick Ge well embedded inside the Si_{0.5}Ge_{0.5} alloy barrier, we construct a supercell containing a 140 monolayer (ML) Ge well and 70 ML Si_{0.5}Ge_{0.5} alloy barrier which is thick enough to avoid the artificial image interaction caused by periodic boundary condition utilized in the calculation. To capture the randomness of atomic alloy configurations in the Si_{0.5}Ge_{0.5} alloy barrier, we augment the supercell in the in-plane directions to 5×5 by taking one random configuration for calculation of the electronic structures and thus the spin splitting, where the randomness induced fluctuations are systematically investigated in Ref. [22]. We utilize the atomistic SEPM, which has been broadly used in the electronic structure calculation of quantum structures [30–38], to compute the electronic structures of Ge/SiGe QWs whose relaxed atomic configurations are obtained by minimizing the strain energy using the valence force field method [detailed in Ref. ([17])].

Figure 1 shows the atomistic pseudopotential calculated spin splitting of the first HH subband for the Ge/Si_{0.5}Ge_{0.5} QW with 20 nm thick Ge well upon application of a moderate electric field of 100 kV/cm. Here, the obtained spin splitting is fully caused by Rashba SOC due to the Dresselhaus SOC absent in centrosymmetric Si and Ge. We can formulate the spin splitting using $\Delta E_{SS} = 2\alpha_R k + \gamma_R k^3$, where α_R and γ_R are the k -linear and k -cubic Rashba parameters characterizing the strength of k -linear and k -cubic Rashba SOC, respectively.

We obtain $\alpha_R = 1.6$ meVÅ and $\gamma_R = 1.1$ eVÅ³ after fitting the spin splitting ΔE_{SS} to above formula for $k < 0.01$ ($\frac{2\pi}{a}$). Whereas we get $\alpha_R = 0.8$ meVÅ and $\gamma_R = 9.4$ eVÅ³ if we fit

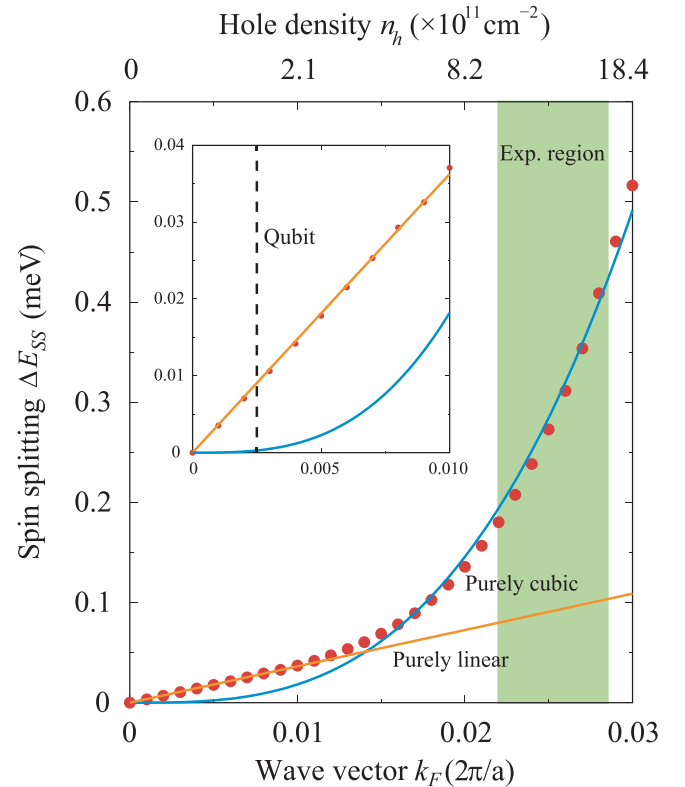


FIG. 1. Direct comparison between SEPM calculation and experimental results. Spin splitting ΔE_{SS} at different Fermi wavevectors k_F along the [100] direction with the lattice constant a being 5.54 Å in the 20 nm strained Ge/Si_{0.5}Ge_{0.5} QW. The red dots denote the SEPM results. The blue and orange lines are the fitting curves of the red dots (SEPM results) fitted by the purely k -cubic term at a large k_F and the purely k -linear term at a small k_F , where the parameters are $\gamma_R = 12.5$ eVÅ³ and $\alpha_R = 1.6$ meVÅ, respectively. The green region shows the Fermi wavevector k_F corresponding to the hole density n_h where the k -cubic Rashba SOC is obtained in the experiment. The inset shows the spin splitting within a smaller k_F range, and the black dashed line represents the Fermi wavevector k_F of 2D gate-defined QDs. The external electric field applied to the Ge QW is 100 kV/cm.

the spin splitting for $k < 0.025(\frac{2\pi}{a})$. The remarkable change in α_R and γ_R indicates that the spin splitting is highly k -dependent. Indeed, the spin splitting exhibits two different dispersion models: a linear dispersion for $k < 0.01(\frac{2\pi}{a})$ and a sublinear dispersion for $k > 0.015(\frac{2\pi}{a})$.

To demonstrate such two-model dispersion, we fit the spin splitting to a purely k -linear term for $k < 0.01(\frac{2\pi}{a})$ and to a purely k -cubic term for $0.015(\frac{2\pi}{a}) < k < 0.025(\frac{2\pi}{a})$. We obtain $\alpha_R = 1.6$ meVÅ (the orange line as shown in Fig. 1), manifesting a negligible k -cubic term in this k -range. This finite k -linear Rashba SOC originates from a direct dipolar subband coupling induced by the external electric field in the presence of the HH-LH mixing at the Brillouin zone center [17]. We have demonstrated that it offers the fast manipulation of spin qubits in 2D gate-defined Ge quantum dots (QDs) [21], in which the Fermi wavevector k_F was estimated to be $0.0025(\frac{2\pi}{a})$ within the small k -range (the black dashed line in the inset of Fig. 1). Figure 1 shows that, for $0.015(\frac{2\pi}{a}) < k < 0.025(\frac{2\pi}{a})$, we fit the spin splitting well to a purely k -cubic term with $\gamma_R = 12.5$ eVÅ³ (the blue line as shown in Fig. 1), manifesting a negligible k -linear term in this k -range. In the magnetotransport experiment [24], the hole density n_h in the Ge/SiGe QWs is in the range of 10 – 15×10^{11} cm⁻², corresponding to the Fermi wavevector k_F between 0.022 and $0.027(\frac{2\pi}{a})$ (marked by the green area in Fig. 1). At this k -range, our atomistic method predicted Rashba SOC of the first HH subband is indeed k -cubic dominated with a negligible k -linear term. Our predicted $\gamma_R = 12.5$ eVÅ³ is in good agreement with the experimentally deduced values $\gamma_R = 14$ – 20 eVÅ³ [24]. The slight deviation of the k -cubic Rashba parameter γ_R may originate from the inhomogeneity of the electric field provided by the gate voltage in the experiment. To assess the predicted k -linear Rashba SOC, one has to reduce k_F below $0.010 \times (\frac{2\pi}{a})$, as shown in the inset of Fig. 1. It means one has to substantially decrease the hole density to $n_h < 2.1 \times 10^{11}$ cm⁻². Unfortunately, as shown in Table I, all the experiments [24–29] are conducted at a high hole density larger than 2×10^{11} cm⁻², leading to the failure of probing this k -linear Rashba SOC. At this point, we can understand why previous experiments fail to observe the linear Rashba SOC.

III. REPRODUCTION OF THE MAGNETOTRANSPORT EXPERIMENTAL DATA: INCLUDING BOTH LINEAR AND CUBIC TERMS

To further demonstrate it, we now turn to examine the magnetotransport experiment, which utilizes the WL and WAL effects to fit the conductivity change under external magnetic fields [24–29,39–44]. The WL effect originates from the constructive interference of two coherent partial waves of charge carriers propagating along a looping trajectory in opposite directions in disordered systems, leading to an enhanced backscattering and hence suppression of conductivity [39,40]. An external magnetic field will break the constructive interference and enhance the conductivity due to the existence of a phase difference arising from the magnetic flux. In the presence of a strong SOC, the interference of charge carriers will reduce the backscattering, leading to an enhanced con-

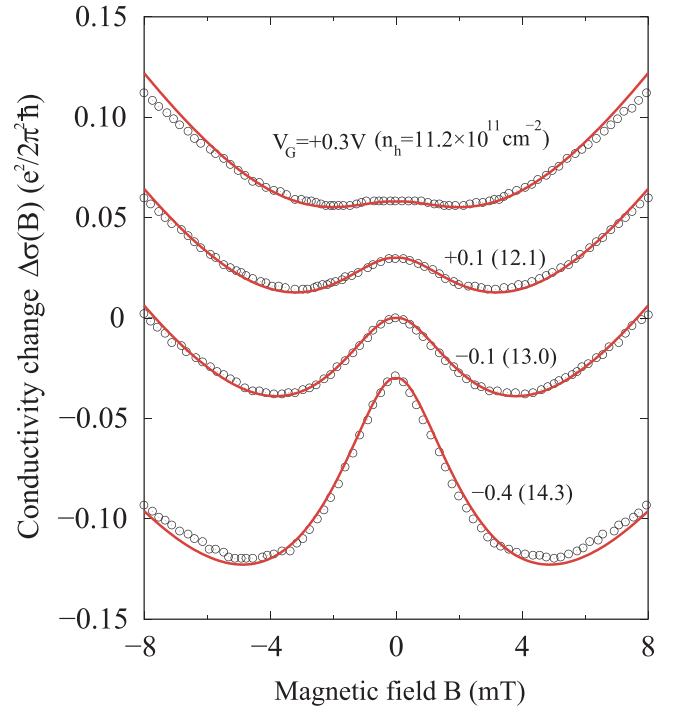


FIG. 2. Conductivity change $\Delta\sigma$ under external magnetic fields B in the strained Ge/Si_{0.5}Ge_{0.5} QW with 20 nm thick in Ge well. The black circles are the experimental data extracted from Ref. ([24]) with the red lines fitted by considering both the k -linear and k -cubic Rashba SOC. The k -cubic Rashba parameters γ_R are 15.3, 15.6, 16.0, and 17.0 eVÅ³ for gate voltage $V_G = -0.4, -0.1, +0.1,$ and $+0.3$ V, respectively, as deduced in Ref. ([24]). The corresponding hole densities are $14.3 \times 10^{11}, 13.0 \times 10^{11}, 12.1 \times 10^{11},$ and 11.2×10^{11} cm⁻², respectively. The utilized k -linear Rashba parameter α_R is 0.8 meVÅ as obtained from our SEPM results at such high hole densities.

ductivity beyond the WL effect, which is called the WAL effect. A peak will appear on the curve of conductivity change as a character of the WAL effect [39,40], as shown in Fig. 2. The WL-WAL effect is described by the Iordanskii, Lyanda-Geller, and Pikus (ILP) model, where the conductivity change $\Delta\sigma$ is a function of four effective magnetic fields: B_ϕ for the characteristic magnetic field for the phase coherence, B_{tr} for the elastic scattering, B_{SO1} for the k -linear SOC, and B_{SO3} for the k -cubic SOC (see Appendix A for details). These four effective magnetic fields are defined as follows [39,40]:

$$\begin{aligned} B_{SO1} &= \frac{4m_h^2\alpha_R^2}{\hbar^3 e}, \\ B_{SO3} &= \frac{4\pi^2\gamma_R^2 m_h^2 n_h^2}{\hbar^3 e}, \\ B_\phi &= \frac{m_h^2}{4\pi\hbar e n_h \tau_\phi}, \\ B_{tr} &= \frac{m_h^2}{4\pi\hbar e n_h \tau_{tr}}, \end{aligned} \quad (1)$$

where, n_h is the hole density, m_h is the hole effective mass, τ_ϕ is the phase coherent time, and τ_{tr} is the elastic scattering time.

In the experimental measurements, B_{tr} is straightforward to obtain since the hole density n_h , effective mass m_h , and elastic scattering time τ_{tr} can be directly measured. One can then acquire B_{SO3} , B_ϕ , and B_{SO1} by fitting the analytic formula of the conductivity change $\Delta\sigma$ to experimentally measured data (See Appendix A for details). Once one gets B_{SO3} and B_{SO1} , it is ready to have the purely k -cubic Rashba parameter γ_R and k -linear Rashba parameter α_R according to Eq. (1). Figure 2 shows the experimentally measured conductivity change $\Delta\sigma$ (the black circles) against the external magnetic field at different hole densities tuned by the gate voltage [24]. Moriya *et al.* have demonstrated [24] that one can only consider k -cubic Rashba SOC in the fitting of conductivity change $\Delta\sigma$ because the k -linear term will make the fitting deviate significantly from the experimental data at the high magnetic field region. From the spin splitting induced by Rashba SOC as shown in Fig. 1, we can now be ready to understand why the experiment fails to probe the k -linear Rashba SOC, regarding the experiment was conducted at high hole densities where the k -cubic Rashba SOC dominates with a negligible k -linear term. Specifically, in the Fermi wavevector range accounting for such high hole densities, our SEPM predicted that the k -linear term becomes very weak with a k -linear Rashba parameter $\alpha_R=0.8$ meVÅ. Figure 2 shows that we can still reproduce well the experimentally measured conductivity change both at low and high magnetic field regions even if we consider such a weak k -linear term (the red lines). Note that in the original experimental paper [24], the conclusion was drawn based on the fitting considering solely either k -linear or k -cubic Rashba SOC term rather than their combination. The detailed fitting parameters are given in Appendix B.

IV. EVALUATION OF THE WEAK-ANTILOCALIZATION EFFECT

The WAL in the magnetotransport arises from a predominant effect of strong SOC in correcting the conductivity change [43]. This is because the negative correction at low magnetic fields will appear if and only if the SOC-induced magnetic field $B_{SO} = B_{SO1} + B_{SO3}$ is so strong that it is larger than the phase coherence field B_ϕ . Otherwise, only the WL effect appears. The WL-WAL transition reflects the appearance and controllability of the SOC, which is an important phenomenon in obtaining the Rashba parameters α_R and γ_R . We define a parameter $r_2 = B_{SO}/B_\phi$ to characterize the WL-WAL transition: $r_2 < 1$ indicates the WL effect and $r_2 > 1$ represents the WAL effect. The hole density plays an essential role in this transition via controlling the SOC strength. As shown in Fig. 2, the WAL effect diminishes and finally transforms into the WL effect with the reduction of the hole density.

We have demonstrated that experiments can only detect the linear Rashba SOC at low hole densities. The key question is whether it is possible to have the WAL at low hole densities in Ge QWs. To address this issue we examine the WL-WAL transition by varying the hole density n_h . To do it, we rewrite r_2 as

$$r_2 = \frac{16\pi\tau_{tr}\tau_\phi n_h}{\hbar^2} (\alpha_R^2 + \pi^2 n_h^2 \gamma_R^2), \quad (2)$$

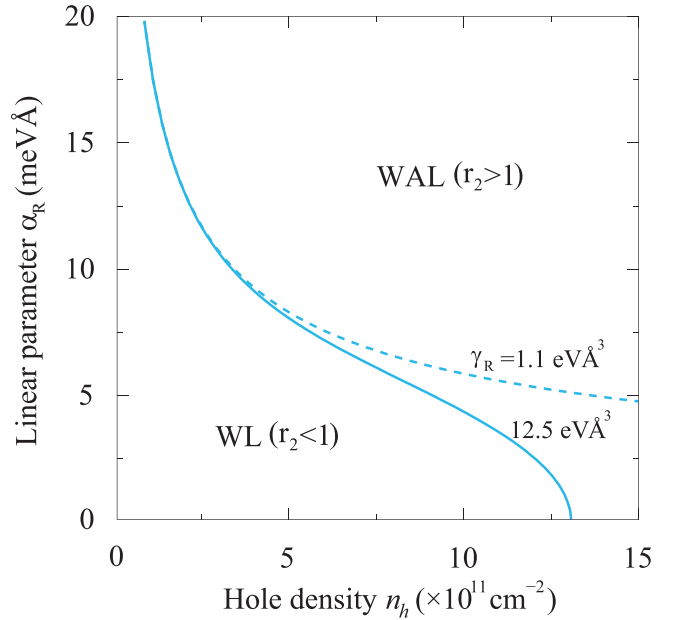


FIG. 3. Dependence of the WAL and WL regimes as characterized by the parameter $r_2 = B_{SO}/B_\phi$ on the hole density n_h and k -linear Rashba parameter α_R . The blue lines represent the WL-WAL transition ($r_2 = 1$) by fixing the k -cubic Rashba parameter γ_R to 12.5 eVÅ³ (the solid line) and 1.1 eVÅ³ (the dashed line), respectively. We set $\tau_{tr} \times \tau_\phi = 2.5$ ps².

and change hole density n_h and the k -linear Rashba parameter α_R but fix the k -cubic Rashba parameter γ_R and the product of the elastic scattering and phase coherent time τ_{tr} and τ_ϕ . Figure 3 shows that the WL-WAL transition ($r_2=1$, see the blue lines) could occur at both high ($n_h > 10 \times 10^{11}$ cm⁻²) and low hole densities ($n_h < 3 \times 10^{11}$ cm⁻²) as varying α_R . Specifically, as reducing the hole density n_h , the k -linear Rashba parameter α_R has to be increased to achieve the WAL. As we discussed above, in the investigated Ge QW the k -linear term becomes visible and dominant over the k -cubic term only when the hole density is smaller than 2.1×10^{11} cm⁻² with regard to the high k -dependent Rashba SOC in 2D holes. The corresponding k -linear Rashba parameter α_R is 1.6 meVÅ, which is too small to achieve the WAL, as shown in Fig. 3, unless one increases the hole density n_h to, for example, 12.6×10^{11} cm⁻² in which the k -cubic Rashba SOC was found to be around $\gamma_R = 12.5$ eVÅ³ (see the blue solid line). Hence we observe the WL-WAL transition in Fig. 2. Whereas if the k -cubic Rashba SOC is also weak, e.g., $\gamma_R=1.1$ eVÅ³, the WAL will never appear even at high hole densities, unless one could enhance the k -linear Rashba parameter α_R above 4.7 meVÅ (see the blue dashed line). Figure 3 shows that to achieve the WAL at the hole density n_h of 2.1×10^{11} cm⁻² one has to enhance the k -linear Rashba parameter α_R above 12.6 meVÅ. One could vary the QW orientation to, for example, [110] direction [17,23], and engineer the barrier potential [22] to significantly enhance the k -linear Rashba parameter α_R in 2D holes. Note that the k -cubic Rashba SOC has negligible effects in the WL-WAL transition at low hole densities. We also discuss the conductivity change in different ratios of k -linear and k -cubic terms in Appendix C.

TABLE II. Fitting parameters of four characteristic magnetic fields B_{SO1} , B_{SO3} , B_ϕ , and B_{tr} for the conductivity change in Fig. 2 in the main text.

Gate voltage (V)	B_{SO1} (mT)	B_{SO3} (mT)	B_ϕ (mT)	B_{tr} (mT)	$r_2 = \frac{(B_{SO1}+B_{SO3})}{B_\phi}$
-0.4	0.0190	1.40	0.72	28.69	1.98
-0.1	0.0200	1.27	0.94	39.14	1.37
+0.1	0.0214	1.24	1.17	59.71	1.08
+0.3	0.0205	1.14	1.48	75.98	0.79

We notice that 2D electrons in narrow bandgap semiconductor quantum wells usually have such a strong k -linear Rashba SOC, that it is large enough to be probed frequently in experiments. For example, Koga *et al.* deduced experimentally the k -linear Rashba parameter α_R being 12 to 40 meVÅ from the WAL in InGaAs/InAlAs QWs [43]. It is interesting to note that for $\alpha_R = 2$ meVÅ they could only observe the WL at electron density of 7×10^{11} cm⁻². The large change in α_R might be attributed to the k -linear Rashba SOC in 2D electrons being regulated by interface [45] and gate voltage.

V. CONCLUSION

In summary, we explain why experiments fail to probe the recently found k -linear Rashba SOC. We illustrate that the hole densities involved in the experiments are so high that the emerging k -linear term becomes negligible and the highly k -dependent Rashba SOC becomes almost purely k -cubic. We demonstrate that the k -linear term must be larger than 4.7 meVÅ to be detectable at high hole densities in magnetotransport experiments. We also evaluate the possibility of achieving the WAL at low hole densities. This work bridges the theoretically discovered k -linear term and the experimentally observed k -cubic term alone for Rashba SOC in 2D holes.

ACKNOWLEDGMENTS

This work was supported by the National Science Fund for Distinguished Young Scholars under Grant No. 11925407, the Basic Science Center Program of the National Natural Science Foundation of China (NSFC) under Grant No. 61888102, and the Key Research Program of Frontier Sciences, CAS under Grant No. ZDBS-LY-JSC019. S. G. was also supported by the NSFC under Grant No. 11904359.

APPENDIX A: EXPRESSION OF THE CONDUCTIVITY CHANGE UNDER EXTERNAL MAGNETIC FIELDS IN THE ILP MODEL

In the ILP model, the conductivity change can be written as [7,24,39,40]

$$\begin{aligned} \Delta\sigma(B) &= -\frac{e^2}{4\pi^2\hbar} \left[\frac{1}{a_0} + \frac{2a_0 + 1 + \frac{B_{SO1}+B_{SO3}}{B}}{a_1(a_0 + \frac{B_{SO1}+B_{SO3}}{B}) - 2\frac{B_{SO1}}{B}} \right. \\ &\quad \left. - \sum_{n=1}^{\infty} \left\{ \frac{3}{n} - \frac{3a_n^2 + 2a_n\frac{B_{SO1}+B_{SO3}}{B} - 1 - 2(2n+1)\frac{B_{SO1}}{B}}{(a_n + \frac{B_{SO1}+B_{SO3}}{B})a_{n-1}a_{n+1} - 2\frac{B_{SO1}}{B}[(2n+1)a_n - 1]} \right\} \right. \\ &\quad \left. + 2\ln\left(\frac{B_{tr}}{B}\right) + \Psi\left(\frac{1}{2} + \frac{B_\phi}{B}\right) + 3C \right], \end{aligned} \quad (A1)$$

where the parameters are

$$\begin{aligned} a_n &= n + \frac{1}{2} + \frac{B_\phi}{B} + \frac{B_{SO1} + B_{SO3}}{B}, \\ B_{SO1} &= \frac{\hbar}{4eD} 2|\Omega_1|^2 \tau_{tr}, \\ B_{SO3} &= \frac{\hbar}{4eD} 2|\Omega_3|^2 \tau_{tr}, \\ B_\phi &= \frac{\hbar}{4eD\tau_\phi}, \\ B_{tr} &= \frac{\hbar}{4eD\tau_{tr}}. \end{aligned} \quad (A2)$$

Here Ψ is the digamma function, C is the Euler constant, e is the electron charge, \hbar is the reduced Plank's constant, D is the diffusion constant, τ_ϕ is the phase coherent time of the carrier, and τ_{tr} is the elastic scattering time. The parameter B_{SO1} (B_{SO3}) is the k -linear Ω_1 (k -cubic Ω_3) effective mag-

TABLE III. Fitting parameters n_h , k_F , m_h , τ_{tr} , τ_ϕ , α_R , and γ_R for the conductivity change in Fig. 2 in the main text.

Gate voltage (V)	n_h (10^{11} cm ⁻²)	k_F ($\frac{2\pi}{a}$)	m_h (m_0)	τ_{tr} (ps)	τ_ϕ (ps)	α_R (meVÅ)	γ_R (eVÅ ³)
-0.4	14.3	0.0264	0.081	0.25	9.96	0.8	15.3
-0.1	13.0	0.0256	0.083	0.23	9.58	0.8	15.6
+0.1	12.1	0.0247	0.086	0.20	10.21	0.8	16.0
+0.3	11.2	0.0238	0.084	0.18	9.24	0.8	17.0

netic field in frequency unit, B_ϕ and B_{lr} are the characteristic magnetic fields for the phase coherence and the elastic scattering, respectively. When the external magnetic field B is much smaller than the characteristic magnetic field for the elastic scattering B_{lr} , the magnetotransport is in the diffusive region, where the Rashba parameters are obtained by fitting the conductivity change against B according to Eq. (A1) in experiments. The k -linear (k -cubic) spin splitting $\Delta E_{SS1} = \hbar|\Omega_1|$ ($\Delta E_{SS3} = \hbar|\Omega_3|$) is equal to $\Delta E_{SS1} = 2\alpha_R k_F$ ($\Delta E_{SS3} = \gamma_R k_F^3$), where α_R (γ_R) is the k -linear (k -cubic) parameter and k_F is the Fermi wavevector determined by the hole density n_h . The diffusion constant $D = \frac{v_F^2 \tau_{lr}}{2}$ is related to the Fermi velocity v_F , where $v_F = \frac{\hbar k_F}{m_h}$. Thus, according to Eq. (A2), we can obtain Eq. (2) in the main text.

From Eqs. (A1) and (A2), we learn that the conductivity change $\Delta\sigma(B)$ is determined by four parameters of characteristic magnetic fields B_{SO1} , B_{SO3} , B_ϕ , and B_{lr} . These four parameters can be further expressed as functions of the k -linear and k -cubic Rashba (or Dresselhaus) parameters α_R and γ_R , the elastic scattering time τ_{lr} and the phase coherent time τ_ϕ , the hole effective mass m_h , and the hole density n_h . A large hole density n_h will result in a small k -linear Rashba parameter α_R and a large k -cubic Rashba parameter γ_R . Hence Rashba parameters α_R and γ_R are related to the hole density n_h . Furthermore, since τ_{lr} , τ_ϕ , and m_h (actually m_h changes little at different hole density) are also influenced by the hole density n_h , the hole density n_h lies in the central position in the conductivity change $\Delta\sigma(B)$.

APPENDIX B: FITTING PARAMETERS OF THE CONDUCTIVITY CHANGE

The fitting parameters of the conductivity change in the figures of the main text are given here. Table II and Table III show the parameters of Fig. 2 in the main text.

APPENDIX C: CONDUCTIVITY CHANGE AT DIFFERENT RATIOS OF k -LINEAR AND k -CUBIC TERMS

The conductivity changes have different curve shapes at different ratios of k -linear and k -cubic Rashba terms. Hence

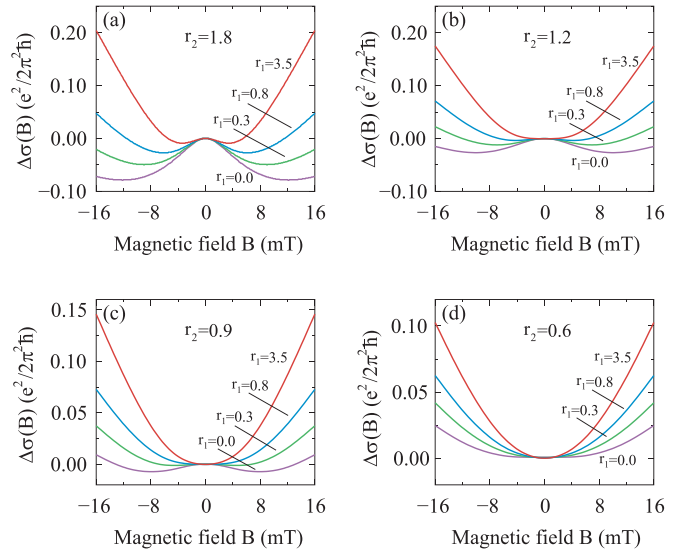


FIG. 4. Conductivity change $\Delta\sigma$ under external magnetic fields B with different parameters $r_1 = \frac{B_{SO1}}{B_{SO3}}$ and $r_2 = \frac{B_{SO}}{B_\phi}$. We keep $B_{SO}=3.6$ mT unchanged and change B_ϕ in (a) $B_\phi=2.0$ mT ($r_2=1.8$), (b) $B_\phi=3.0$ mT ($r_2=1.2$), (c) $B_\phi=4.0$ mT ($r_2=0.9$), and (d) $B_\phi=6.0$ mT ($r_2=0.6$). The red, blue, green, and purple lines denote $r_1=3.5$ (k -linear term dominates), 0.8, 0.3, and 0.0 (purely k -cubic SOC), respectively. Here we set $B_{lr}=40.0$ mT, which is much larger than external magnetic fields.

we can define $r_1 = \frac{B_{SO1}}{B_{SO3}}$ to describe their competition. Figure 4 shows the conductivity change at different r_1 with r_2 fixed, where we keep B_{SO} unchanged and change B_ϕ . A large r_1 increases the slope of the conductivity change at high magnetic fields and suppresses the WAL effect [Fig. 4(a)–4(c)] or enhances the WL effect [Fig. 4(d)]. From Fig. 4(a) to Fig. 4(d), the conductivity change diminishes with the reduction of r_2 . Because the parameter r_1 can be further written as

$$r_1 = \frac{\alpha_R^2}{\pi^2 n_h^2 \gamma_R^2}, \quad (C1)$$

a low hole density n_h in a combination of a large k -linear Rashba parameter α_R and a small k -cubic Rashba parameter γ_R will increase the slope of the conductivity change.

[1] Yu. A. Bychkov and É. I. Rashba, *JETP Lett.* **39**, 78 (1984).
[2] R. Winkler, *Phys. Rev. B* **62**, 4245 (2000).
[3] R. Winkler, *Spin-Orbit Coupling Effect in Two-Dimensional Electron and Hole Systems* (Springer, Berlin, Heidelberg, 2003), Chap. 6, pp. 59–129.
[4] E. Marcellina, A. R. Hamilton, R. Winkler, and D. Culcer, *Phys. Rev. B* **95**, 075305 (2017).
[5] D. V. Bulaev and D. Loss, *Phys. Rev. Lett.* **95**, 076805 (2005).
[6] B. A. Bernevig and S.-C. Zhang, *Phys. Rev. Lett.* **95**, 016801 (2005).
[7] H. Nakamura, T. Koga, and T. Kimura, *Phys. Rev. Lett.* **108**, 206601 (2012).
[8] S. Datta and B. Das, *Appl. Phys. Lett.* **56**, 665 (1990).

[9] J. Schliemann, J. C. Egues, and D. Loss, *Phys. Rev. Lett.* **90**, 146801 (2003).
[10] I. Žutić, J. Fabian, and S. Das Sarma, *Rev. Mod. Phys.* **76**, 323 (2004).
[11] J. Schliemann and D. Loss, *Phys. Rev. B* **69**, 165315 (2004).
[12] J. Sinova, D. Culcer, Q. Niu, N. A. Sinitsyn, T. Jungwirth, and A. H. MacDonald, *Phys. Rev. Lett.* **92**, 126603 (2004).
[13] Y. K. Kato, R. C. Myers, A. C. Gossard, and D. D. Awschalom, *Science* **306**, 1910 (2004).
[14] J. Schliemann and D. Loss, *Phys. Rev. B* **71**, 085308 (2005).
[15] J. Wunderlich, B.-G. Park, A. C. Irvine, L. P. Zárbo, E. Rozkotová, P. Nemeč, V. Novák, J. Sinova, and T. Jungwirth, *Science* **330**, 1801 (2010).

- [16] X. Bi, P. He, E. M. Hankiewicz, R. Winkler, G. Vignale, and D. Culcer, *Phys. Rev. B* **88**, 035316 (2013).
- [17] J.-X. Xiong, S. Guan, J.-W. Luo, and S.-S. Li, *Phys. Rev. B* **103**, 085309 (2021).
- [18] N. W. Hendrickx, D. P. Franke, A. Sammak, M. Kouwenhoven, D. Sabbagh, L. Yeoh, R. Li, M. L. V. Tagliaferri, M. Virgilio, G. Capellini *et al.*, *Nat. Commun.* **9**, 2835 (2018).
- [19] N. W. Hendrickx, D. P. Franke, A. Sammak, G. Scappucci, and M. Veldhorst, *Nature (London)* **577**, 487 (2020).
- [20] N. W. Hendrickx, W. I. L. Lawrie, M. Russ, F. van Riggelen, S. L. de Snoo, R. N. Schouten, A. Sammak, G. Scappucci, and M. Veldhorst, *Nature (London)* **591**, 580 (2021).
- [21] Y. Liu, J.-X. Xiong, Z. Wang, W.-L. Ma, S. Guan, J.-W. Luo, and S.-S. Li, *Phys. Rev. B* **105**, 075313 (2022).
- [22] J.-X. Xiong *et al.* (unpublished).
- [23] J.-X. Xiong, S. Guan, J.-W. Luo, and S.-S. Li, *Phys. Rev. B* **105**, 115303 (2022).
- [24] R. Moriya, K. Sawano, Y. Hoshi, S. Masubuchi, Y. Shiraki, A. Wild, C. Neumann, G. Abstreiter, D. Bougeard, T. Koga *et al.*, *Phys. Rev. Lett.* **113**, 086601 (2014).
- [25] C.-T. Chou, N. T. Jacobson, J. E. Moussa, A. D. Baczewski, Y. Chuang, C.-Y. Liu, J.-Y. Li, and T. M. Lu, *Nanoscale* **10**, 20559 (2018).
- [26] C. Morrison, P. Wisniewski, S. D. Rhead, J. Foronda, D. R. Leadley, and M. Myronov, *Appl. Phys. Lett.* **105**, 182401 (2014).
- [27] J. Foronda, C. Morrison, J. E. Halpin, S. D. Rhead, and M. Myronov, *J. Phys.: Condens. Matter* **27**, 022201 (2015).
- [28] C. Morrison, J. Foronda, P. Wisniewski, S. D. Rhead, D. R. Leadley, and M. Myronov, *Thin Solid Films* **602**, 84 (2016).
- [29] M. Failla, M. Myronov, C. Morrison, D. R. Leadley, and J. Lloyd-Hughes, *Phys. Rev. B* **92**, 045303 (2015).
- [30] M. d’Avezac, J.-W. Luo, T. Chanier, and A. Zunger, *Phys. Rev. Lett.* **108**, 027401 (2012).
- [31] L.-J. Zhang, M. d’Avezac, J.-W. Luo, and A. Zunger, *Nano Lett.* **12**, 984 (2012).
- [32] J.-W. Luo, G. Bester, and A. Zunger, *Phys. Rev. B* **92**, 165301 (2015).
- [33] J.-W. Luo, S.-S. Li, and A. Zunger, *Phys. Rev. Lett.* **119**, 126401 (2017).
- [34] J.-W. Luo, G. Bester, and A. Zunger, *Phys. Rev. Lett.* **102**, 056405 (2009).
- [35] J.-W. Luo, A. N. Chantis, M. van Schilfgaarde, G. Bester, and A. Zunger, *Phys. Rev. Lett.* **104**, 066405 (2010).
- [36] J.-W. Luo and A. Zunger, *Phys. Rev. Lett.* **105**, 176805 (2010).
- [37] J.-W. Luo, L. Zhang, and A. Zunger, *Phys. Rev. B* **84**, 121303 (2011).
- [38] J.-W. Luo, S.-S. Li, I. Sychugov, F. Pevero, J. Linnros, and A. Zunger, *Nat. Nanotechnol.* **12**, 930 (2017).
- [39] S. V. Lordanskii, Y. B. Lyanda-Geller, and G. E. Pikus, *JETP Lett.* **60**, 206 (1994).
- [40] W. Knap, C. Skierbiszewski, A. Zduniak, E. L. Staszewska, D. Bertho, F. Kobbi, J. L. Robert, G. E. Pikus, F. G. Pikus, S. V. Iordanskii *et al.*, *Phys. Rev. B* **53**, 3912 (1996).
- [41] F. Herling, C. Morrison, C. S. Knox, S. Zhang, O. Newell, M. Myronov, E. H. Linfield, and C. H. Marrows, *Phys. Rev. B* **95**, 155307 (2017).
- [42] R. L. Kallaher, J. J. Heremans, N. Goel, S. J. Chung, and M. B. Santos, *Phys. Rev. B* **81**, 075303 (2010).
- [43] T. Koga, J. Nitta, T. Akazaki, and H. Takayanagi, *Phys. Rev. Lett.* **89**, 046801 (2002).
- [44] D. C. Marinescu, P. J. Weigele, D. M. Zumbühl, and J. C. Egues, *Phys. Rev. Lett.* **122**, 156601 (2019).
- [45] Y. Hao, C. Yonghai, H. Guodong, and W. Zhanguo, *J. Semicond.* **30**, 062001 (2009).